Supplementary information for
Towards reliable electrical measurements of superconducting devices inside a transmission electron microscope

Joachim Dahl Thomsen[a], Michael I. Faley[a], Joseph Vimal Vas[a], Alexander Clausen[a], Thibaud Denneulin[a], Dominik Biscette[b], Denys Sutter[b], Peng-Han Lu[a], and Rafal E. Dunin-Borkowski[a]

[a]*Ernst Ruska-Centre for Microscopy and Spectroscopy with Electrons, Forschungszentrum Jülich, Germany*
[b]*condenZero AG, 8050 Zürich, Switzerland*

Table of contents:

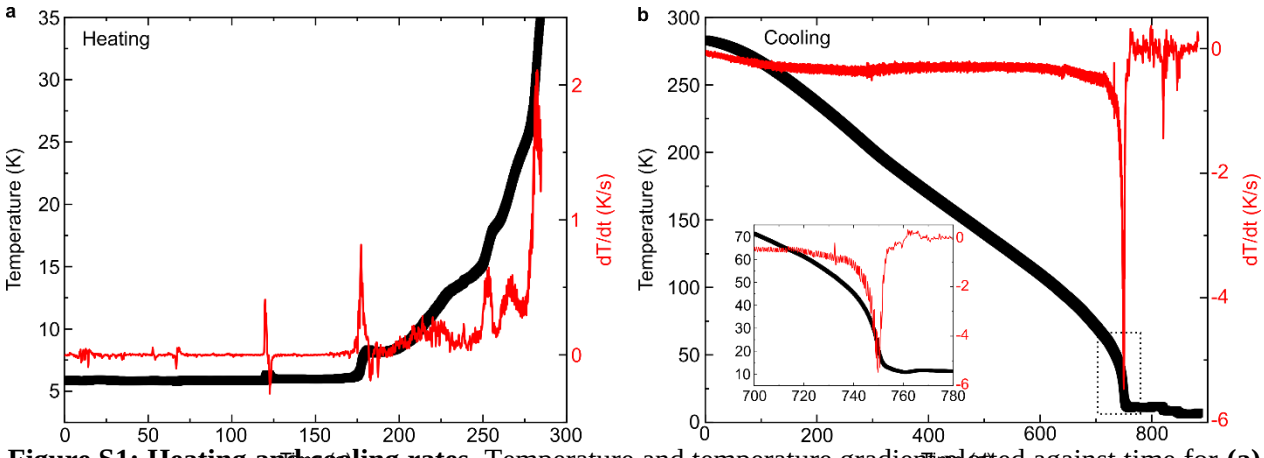

Figure S1: Heating and cooling rates. Temperature and temperature gradient plotted against time for **(a)** heating and **(b)** cooling. We typically used over-pressures of 200-400 mbar for cooling while for heating we slowly vented the helium dewar until the temperature started increase – typically at pressures below 100 mbar.

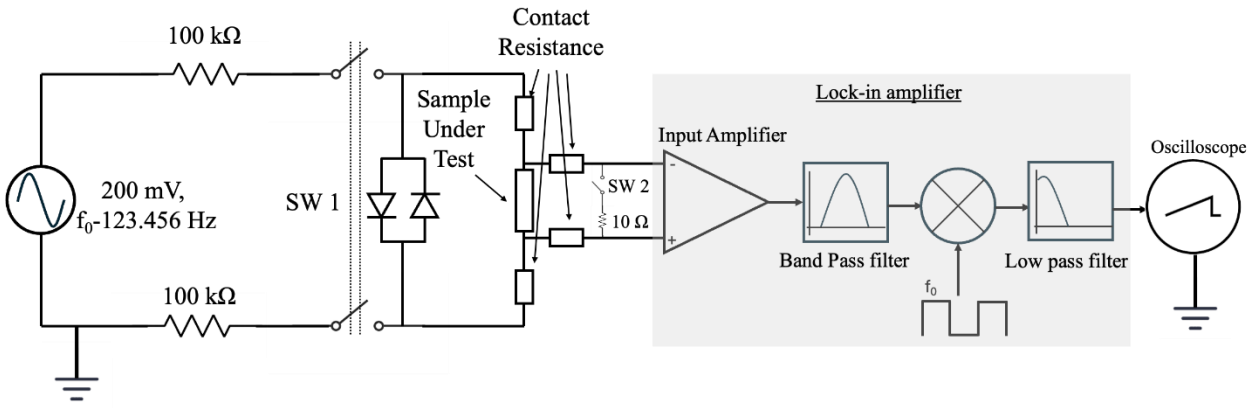

Figure S2: Circuit diagram for the electrical measurement setup. SW=switch. The figure includes an optional oscilloscope which can be used to monitor the AC signal on the sample.

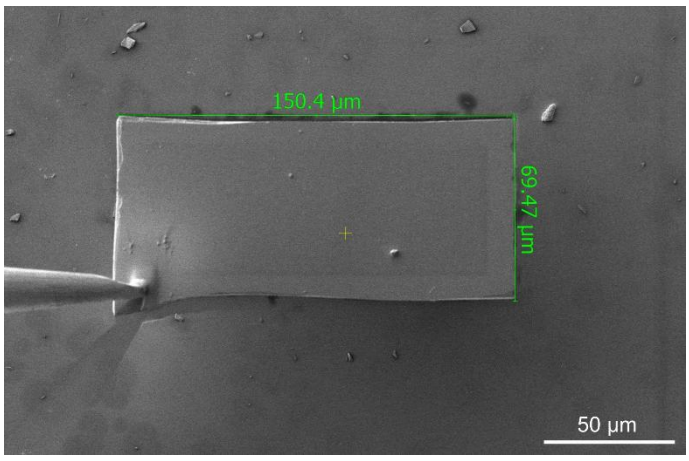

Figure S3: NbN flake overview. SEM image of the NbN flake used for sample 1 during pick up using the nanomanipulator in a TFS Hydra dual beam plasma-focused ion beam (FIB) system.

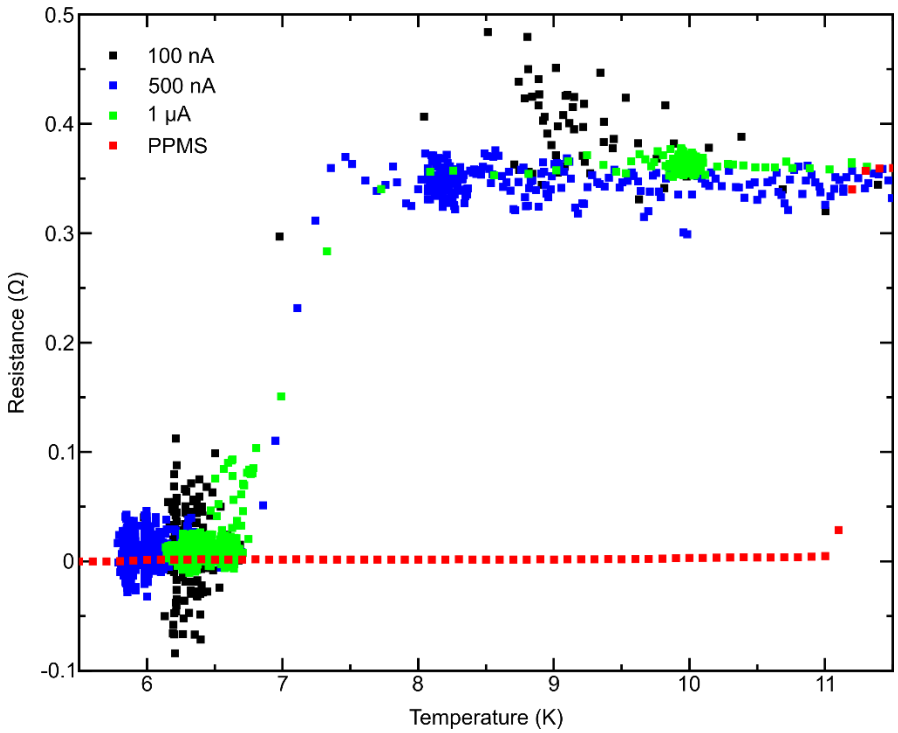

Figure S4: Effect of test current. Resistance of NbN device 1 plotted against temperature, measured in the TEM with the modified cryo-shield with test currents of 100 nA (black), 500 nA (blue), and 1 μA (green). We do not observe any noticeable effect on the apparent T_C^*, other than decreased noise in the resistance measurement.

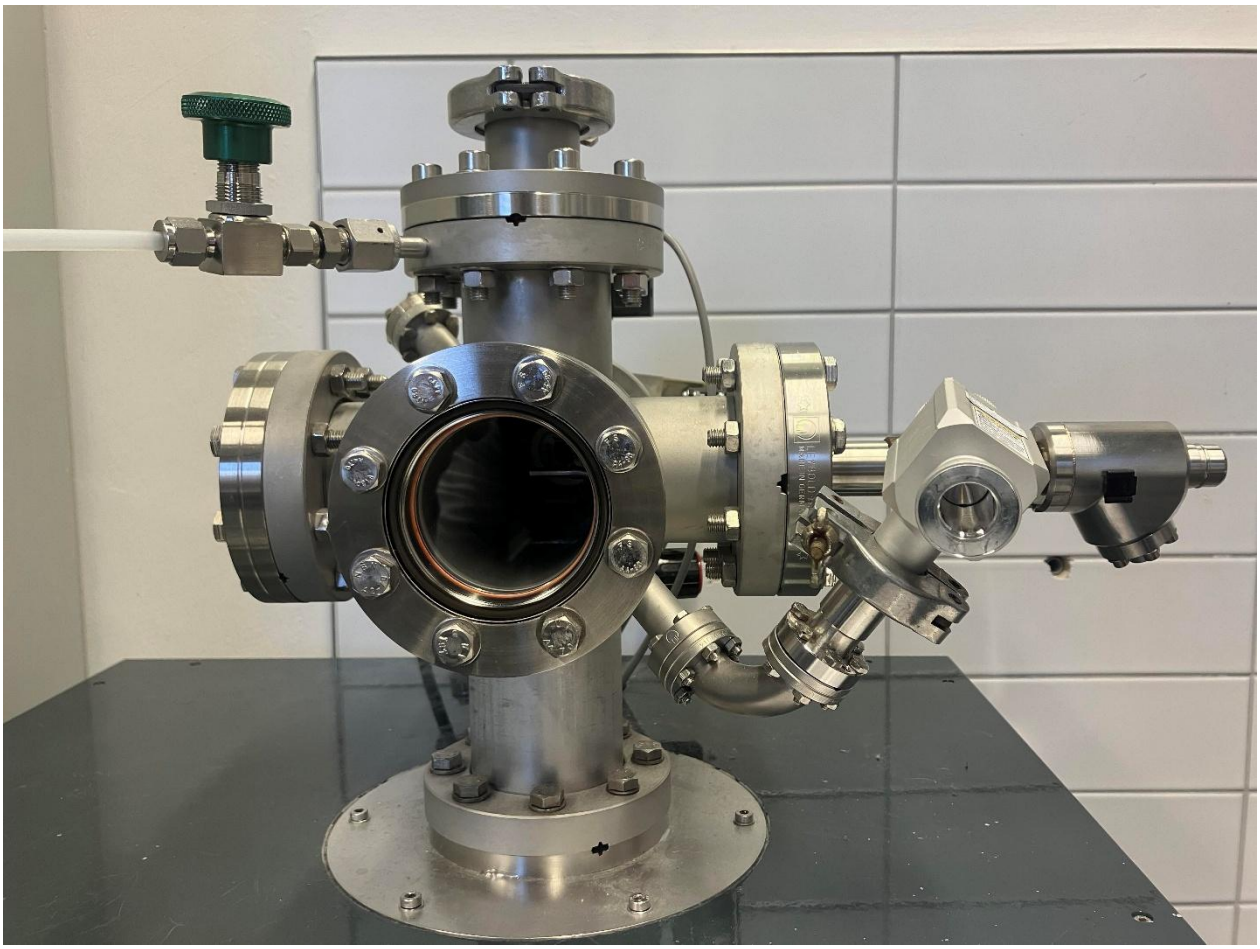

Figure S5: Photograph of the vacuum chamber and sample holder. The connections for electrical measurements and the helium line are not attached.

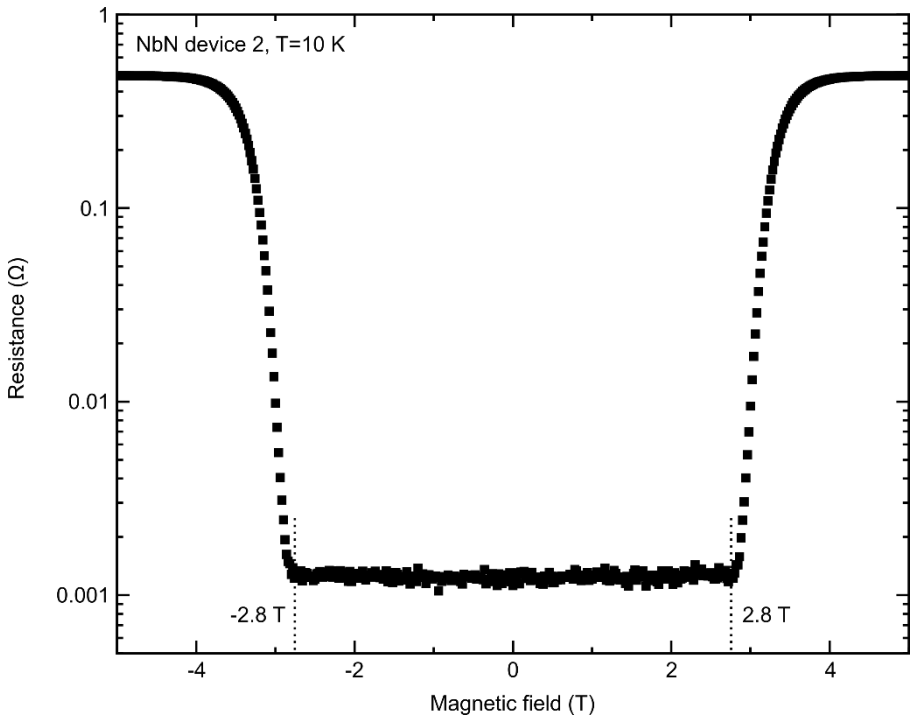

Figure S6: Additional transport data for NbN device 2. PPMS measurement of the resistance of NbN device 2 as a function of applied out-of-plane magnetic field at a constant temperature of 10 K. The vertical dotted lines indicate the critical magnetic field of ±2.8 T.

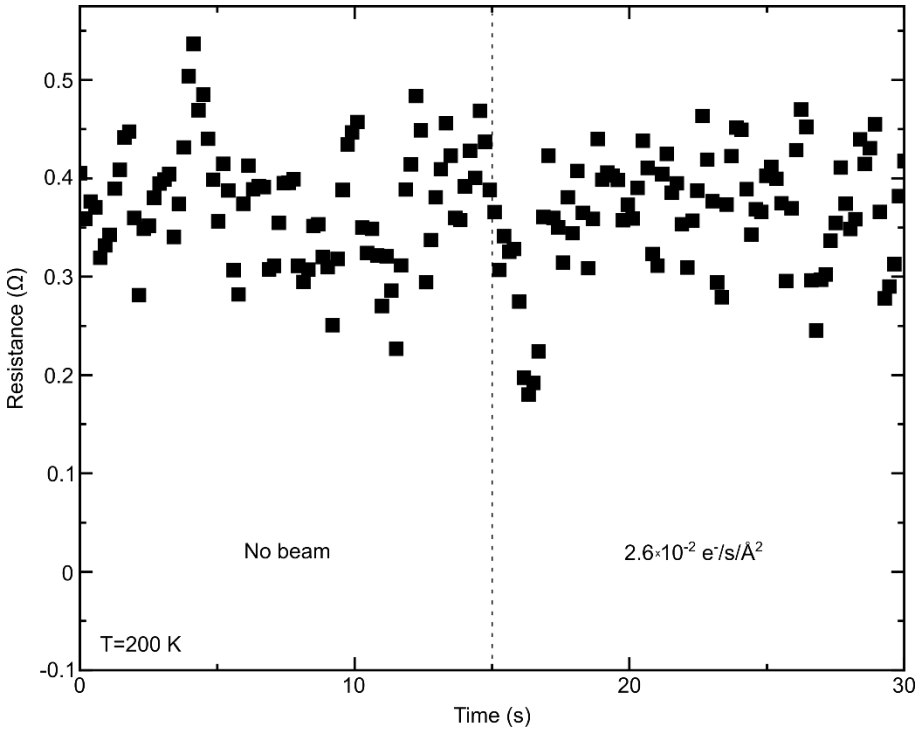

Figure S7: Beam effects above T_c. Resistance plotted against time during an experiment conducted at approximately 200 K. During the first and second 15 s the electron beam was blanked and unblanked with a current density of 2.6×10^{-2} $e^{-}s^{-1}Å^{2}$, respectively. We do not observe a noticeable effect on the resistance at this temperature and with the tested beam current density. This indicates that the resistance changed observed at low temperature are not due to beam-induced doping or charging effects.

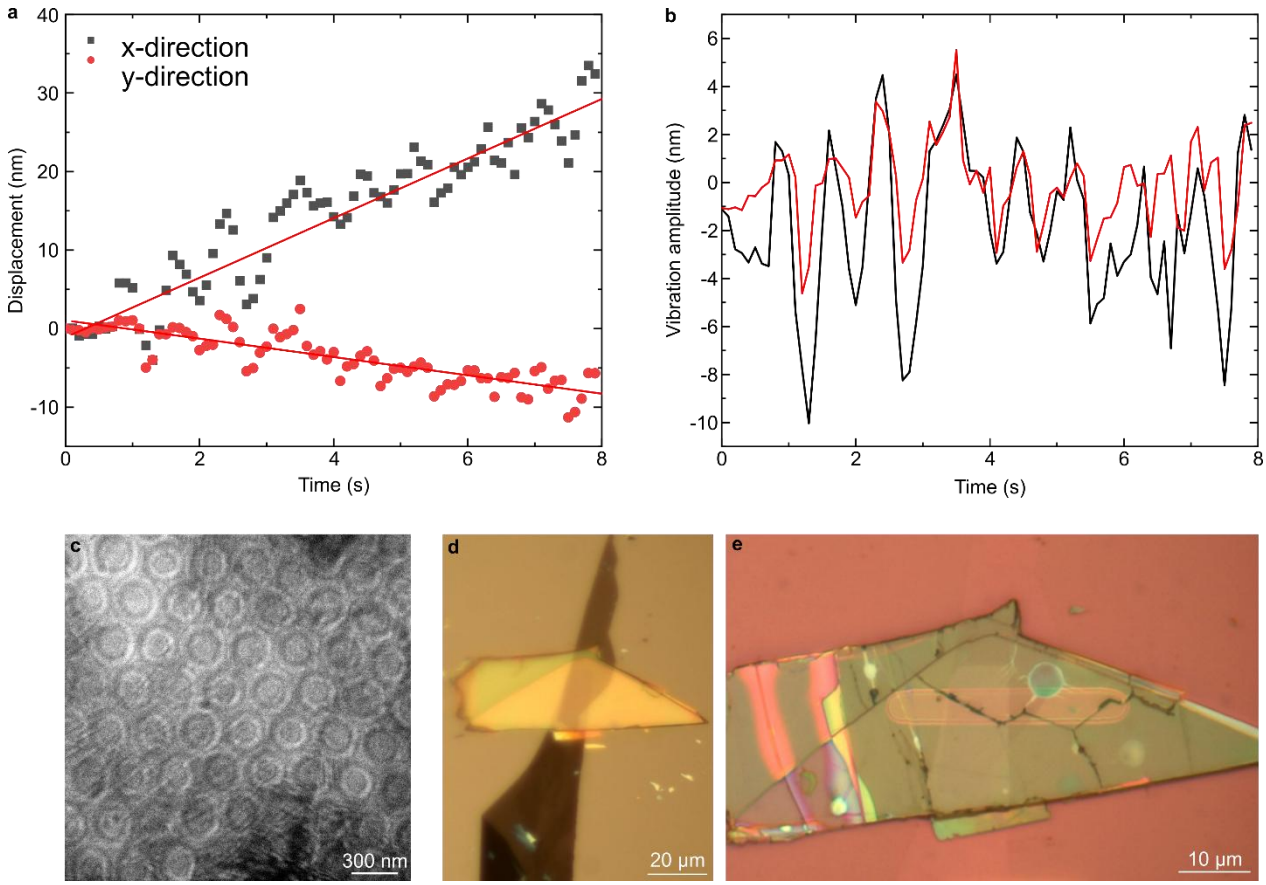

Figure S8: Imaging capabilities and mechanical stability of the sample holder. (a) sample displacement plotted against time, measured from Supplementary Video 1. The red lines are linear fits to the data with slopes of 3.7 nm/s and -1.2 nm/s in the x- and y-direction, respectively. **(b)** Vibration amplitudes plotted against time. The vibration amplitudes are calculated by subtracting the linear fits in (a) to the data. The plot in (b) therefore shows the deviations from the linear sample drift. The standard deviation of this data is 3.2 nm and 1.8 nm in the x- and y-direction, respectively. **(c)** Lorentz TEM image of $CrBr_3$ obtained at a thermometer reading of ~9 K and a defocus of 0.8 mm. A skyrmion lattice is observed after a field cooling process with an applied magnetic field of 50 mT. After reaching the base temperature, the magnetic field is removed. This image is an average of 5 successive images from the time series. Each image in the time series is acquired with an exposure time of 0.1 s. Therefore, the combined exposure time for (c) is 0.5 s. **(d, e)** Optical microscopy images of the sample, after (d) heterostructure assembly and (e) after transfer to the TEM grid. The central region of the $CrBr_3$ flake is encapsulated by few-layer graphene to protect against oxidation.

Supplementary Note 1 - Derivation of the view factor, Eq. 3 in the main text:

The view factor is given by [1]

$$F_{1\to 2} = \frac{1}{A_1}\int_{A_1}\int_{A_2} \frac{\cos\theta_1 \cos\theta_2}{\pi s^2}\,\mathrm{d}A_2\mathrm{d}A_1,$$

where θ_1 and θ_2 are the angles between the surface normal and the line connecting the differential areas, and s is the distance between the two differential areas. Assuming that the device is a point-like object facing a parallel circular disk of radius ρ a distance L away, we have $\cos\theta_1 = \cos\theta_2 = \frac{L}{s}$, with $s = \sqrt{L^2+\rho^2}$. The integral thus reduces to

$$F_{1\to 2} = \int \frac{(L/s)(L/s)}{\pi s^2}\,\mathrm{d}A = \frac{1}{\pi}\int \frac{L^2}{s^4}\,\mathrm{d}A.$$

Using polar coordinates $\mathrm{d}A = \rho\mathrm{d}\rho\mathrm{d}\varphi$ results in

$$F_{1\to 2} = \frac{1}{\pi}\int_0^{2\pi}\int_0^{r} \frac{L^2\rho}{(L^2+\rho^2)}\,\mathrm{d}\rho\mathrm{d}\varphi = \frac{r^2}{L^2+r^2}.$$

The integral is solved by substitution, using $u = L^2+\rho^2 \Rightarrow \mathrm{d}u = 2\rho\mathrm{d}\rho \Rightarrow \rho\mathrm{d}\rho = \frac{du}{2}$.

Supplementary Note 2 – Information about Supplementary Video 1

The video is a time series of Lorentz TEM images obtained at a thermometer reading of ~9 K with the regular cryo-shield, a defocus of 0.8 mm, and zero nominal sample tilt. The time series consists of 80 images, acquired with an exposure time of 0.1 s. The video is shown in real-time, i.e., 10 images per second, and has not been drift corrected. A 2 pixel median filter has been applied to each image. The scale bar is 300 nm.

References

1. Incropera, F. P., Dewitt, D. P., Bergman, T. L. & Lavine, A. S. Principles of heat and mass transfer. (Wiley & Sons Ltd) (2013).